Available online at www.sciencedirect.com
ScienceDirect
Journal of Nutritional Biochemistry 21 (2010) 55–65
Journal of Nutritional Biochemistry

# Licorice isoliquiritigenin dampens angiogenic activity via inhibition of MAPK-responsive signaling pathways leading to induction of matrix metalloproteinases

Sang-Wook Kang[a], Jung-Suk Choi[a], Yean-Jung Choi[a], Ji-Young Bae[a], Jing Li[a], Dong Shoo Kim[a], Jung-Lye Kim[a], Seung-Yong Shin[a], Yong-Jin Lee[b], In-Sook Kwun[c], Young-Hee Kang[a,*]

[a]*Department of Food and Nutrition and Korean Institute of Nutrition, Hallym University, Chuncheon, Kangwon-do, 200-702, South Korea*
[b]*Chuncheon Bioindustry Foundation, Chuncheon, Kangwon-do, 200-702, South Korea*
[c]*Andong University, Andong, Kyeongsangbuk-do, 760-749, South Korea*

Received 21 June 2008; received in revised form 10 September 2008; accepted 3 October 2008

**Abstract**

The aberrant expression of matrix metalloproteinases (MMPs) has been implicated in matrix degradation leading to angiogenesis. This study examined the inhibitory effects of isoliquiritigenin (ISL) on phorbol myristate acetate (PMA)-induced MMP production and its tissue inhibitor of MMP (TIMP) in endothelial cells. No induction of either necrotic or apoptotic cell death was observed in response to a treatment with ISL at ≤25 μM. ISL dose-dependently suppressed PMA-induced expression and activity of MMP-2 and membrane type 1-MMP at ≥1 μM while diminishing the elevated MMP-2 transcript level. In addition, ISL inhibited PMA-triggered migration and tube formation in a dose-dependent manner. ISL further increased the TIMP production up-regulated by PMA with a biphasic effect on TIMP-2 expression. This study further attempted to investigate whether a c-Jun N-terminal kinase (JNK)- or p38 mitogen-activated protein kinase (MAPK)-responsive mechanism was responsible for the MMP production and whether ISL disturbed these signaling pathways. PMA stimulated signaling of JNK and p38 MAPK, which was dampened by ≥10 μM ISL. These results demonstrate that ISL blocked JNK- or p38 MAPK-responsive pathways leading to direct MMP activation of PMA-exposed endothelial cells. Therefore, the ISL inhibition of MMP may boost a therapeutic efficacy during angiogenesis.


*Keywords:* Angiogenesis; Isoliquiritigenin; MMP-2; MT MMP-1; PMA; Tube formation

## 1. Introduction

Matrix metalloproteinases (MMPs) play an important role in tumor invasion, angiogenesis and inflammatory tissue destruction [1,2]. Increased expression of MMP was observed in benign tissue hyperplasia and in atherosclerotic lesions [2,3]. These enzymes may contribute to a cell-invasion-favoring matrix modification and, thus, to an invasive aggressiveness of tumor cells [4,5]. Invasive cancer cells utilize MMP to degrade the extracellular matrix (ECM) and basement membrane during metastasis, and MMP-2 has been implicated in the development and dissemination of malignancies [6]. The interaction between malignant cells and peritumoral benign tissues including the vascular endothelium may serve as an important mechanism in the regulation of tumor invasion and metastasis [6]. Their proteolytic activity is regulated by inhibitors or activators such as tissue inhibitors of MMP (TIMPs), membrane-type MMP (MT MMP) and urokinase-type plasminogen activator (uPA) [1,7,8].

Licorice is a flavorful herb that has been used in food and medicinal remedies for thousands of years. Its root has been used in both Eastern and Western medicine to treat a variety of illnesses ranging from the common cold to liver diseases [9]. Licorice root contains flavonoids such as flavans and chalcones [10–12]. Glabridin, an isoflavan from licorice root, improves survival of mice in an experimental model of septic shock through inhibiting expression of inducible nitric oxide

* Corresponding author. Tel.: +82 33 248 2132; fax: +82 33 254 1475.
*E-mail address:* yhkang@hallym.ac.kr (Y.-H. Kang).

0955-2863/$ – see front matter © 2010 Elsevier Inc. All rights reserved.
doi:10.1016/j.jnutbio.2008.10.004

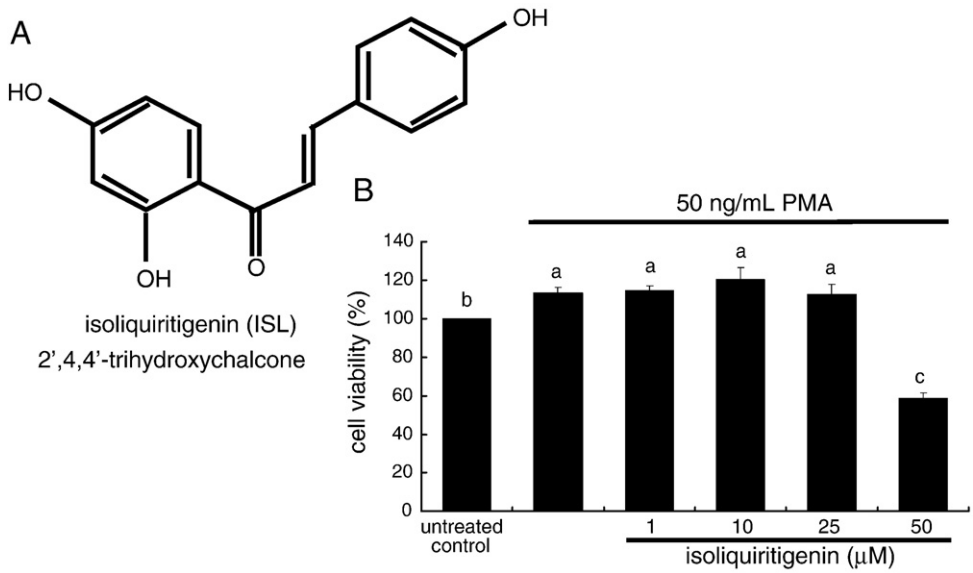


Fig. 1. Chemical structures (A) and cytotoxicity (B) of ISL. After HUVECs were cultured for 24 h in the presence of 50 ng/ml PMA and 1–50 μM ISL, MTT assay was performed. The bar graph data represent means±S.E.M. from five independent experiments with multiple estimations. Values are expressed as percentage of cell survival relative to untreated control cells (cell viability=100%). Values not sharing a letter are different at $P<.05$.

synthase [12]. There is growing interest on the beneficial health effects of isoliquiritigenin (ISL) in licorice root with a chalcone structure, 2′,4,4′-trihydroxychalcone (Fig. 1A), due to its antioxidative, antitumor and anti-inflammatory activities [13,14]. ISL is regarded as a promising potential cancer chemopreventive agent [13,15]. Previous studies have shown that ISL induces apoptosis in colon, gastric and prostate cancer cells [15–17]. However, the antitumor mechanisms of ISL have not been well defined. There is little literature regarding MMP's involvement in matrix modification of ISL as a chemopreventive mechanism.

Licorice-derived flavonoids at micromolar concentrations inhibited tube formation from vascular endothelial cells and granuloma angiogenesis; their potencies for anti-tube formation were in the following order: ISL>isoliquiritin>liquiritigenin≫isoliquiritin apioside [19]. Based on the literature evidence that licorice may inhibit angiogenesis and vascular tumor growth [18,19], the present study determined whether ISL prevents migration and tube formation via inhibition of MMP-2 induction in phorbol 12-myristate 13-acetate (PMA)-exposed human umbilical vein endothelial cells (HUVECs). This study further attempted to elucidate action mechanisms responsible for the MMP activation and for the ISL inhibition of its induction.

## 2. Materials and methods

### 2.1. Materials

M199 medium chemicals, ISL and 3-(4,5-dimetylthiazolyl)-diphenyl tetrazolium bromide (MTT) were obtained from Sigma-Aldrich (St. Louis, MO), as were all other reagents, unless specifically stated elsewhere. Collagenase was purchased from Worthington Biochemicals (Lakewood, NJ). Fetal bovine serum (FBS), penicillin–streptomycin, trypsin–EDTA, human epidermal growth factor and hydrocortisone were purchased from Cambrex (East Rutherford, NJ). Proteins MMP-2 and MT-1 MMP and antibodies against human MMP-2, MT-1 MMP and TIMP-2 were purchased from R&D Systems (Minneapolis, MN). In addition, antibodies against human phospho-c-Jun N-terminal kinase (JNK), human phospho-p38 mitogen-activated protein kinase (MAPK), human phospho-c-Jun and human phospho-p53 were obtained from Cell Signaling Technology (Beverly, MA). Human β-actin antibody was purchased from Sigma Chemicals. Horseradish-peroxidase-conjugated goat anti-rabbit IgG, donkey anti-goat IgG and goat anti-mouse IgG were obtained from Jackson ImmunoResearch Laboratories (West Grove, PA). PMA was purchased from Sigma-Aldrich. Reverse transcriptase, *Taq* DNA polymerase and dNTP were purchased from Promega (Madison, WI). ISL was solubilized in dimethyl sulfoxide (DMSO) for culturing with cells; the final culture concentration of DMSO was ≤0.05%.

### 2.2. Preparation and culture of human endothelial cells

HUVECs were isolated from umbilical cords using collagenase as described elsewhere [14,20]. Cultures were maintained at 37°C humidified atmospheres of 5% $CO_2$ in air. Cells were cultured in 25 mM HEPES-buffered M199 containing 10% FBS, 2 mM glutamine, 100 U/ml penicillin and 100 μg/ml streptomycin supplemented with 0.75 mg/ml human epidermal growth factor and 0.075 mg/ml hydrocortisone.

HUVECs were plated at 90–95% confluence in all experiments. In experiments for the PMA-induced secretion

and expression of MMP-2 and MT-1 MMP, cells were incubated overnight with 1–50 μM ISL prior to an exposure to 50 ng/ml PMA added to serum-free HEPES-buffered M199.

### 2.3. Cell viability assay

At the end of the incubation with ISL in the presence of PMA, MTT assay was performed to quantitate cellular viability [20]. HUVECs were incubated in a fresh medium containing 1 mg/ml MTT for 3 h at 37°C. After removal of unconverted MTT, the purple formazan product was dissolved in 0.5 ml isopropanol through gentle shaking. Absorbance of formazan dye was measured at $\lambda$=570 nm using Bio-Rad Model 550 microplate reader. Nontoxic concentrations of ISL were ≤25 μM for 24-h serum-free culture experiments (Fig. 1A).

### 2.4. Protein isolation and Western blot analysis

Western blot analysis was used to address the fact that 1–25 μM ISL blocked induction of MMP-2, MT-1 MMP and TIMP-2 stimulated by PMA for 24 h. Whole-cell extracts were prepared from HUVECs in 1 M Tris–HCl (pH 6.8) lysis buffer containing 10% SDS, 1% β-glycerophosphate, 0.1 M $Na_3VO_4$, 0.5 M NaF and protease inhibitor cocktail. Cell lysates containing equal amounts of total protein were fractionated by electrophoresis on 10% SDS-PAGE gels and transferred onto a nitrocellulose membrane. Nonspecific binding was blocked by soaking the membrane in TBS-T buffer [0.5 M Tris–HCl (pH 7.5), 1.5 M NaCl and 0.1% Tween 20] containing 5% nonfat dry milk for 3 h. The membrane was incubated overnight with primary monoclonal mouse anti-human antibodies of MMP-2, MT-1 MMP and TIMP-2. After three washes with TBS-T buffer, the membrane was then incubated for 1 h with goat anti-mouse IgG horseradish peroxidase (Jackson ImmunoResearch Laboratories). The protein levels of MMP-2, MT-1 MMP and TIMP-2 were determined by using Supersignal West Pico chemiluminescence detection reagents (Pierce Biotechnology, Rockford, IL) and Konica X-ray film (Konica, Tokyo, Japan). Incubation with monoclonal mouse β-actin antibody was also performed for the comparative control. In order to investigate whether ISL was able to block these MAPK-responsive signaling pathways, we also examined protein levels of phospho-JNK, phospho-p38 MAPK, phospho-c-Jun and phospho-p53 in this study.

### 2.5. Zymography

Inhibition of each activity of MMP-2, MT-1 MMP or TIMP-2 by culturing ISL was determined using different zymography assays.

#### 2.5.1. Gelatin and fibrin zymography

Gelatin zymography of MMP-2 from culture media was performed as previously described [6]. Briefly, culture supernatants were subjected to electrophoresis on 10% SDS-PAGE (0.3 M Tris–HCl, pH 6.8, 4% SDS, 20% glycerol and 0.03% bromophenol blue) copolymerized with 0.1% gelatin as the substrate. For the fibrin zymography measuring MT-1 MMP activity, cell extracts were electrophoresed in gel containing 0.1% fibrinogen and 1 U/ml thrombin. After electrophoresis was complete, the gel was incubated for 1 h at 37°C in a 2.5% Triton X-100 solution, washed in 50 mM Tris–HCl buffer (pH 7.5) for 30 min and incubated for 20 h in 50 mM Tris–HCl buffer (pH 7.5) containing 200 mM NaCl, 10 mM $CaCl_2$ and 0.05% Brij-35. The gel was stained with 0.1% Coomassie Brilliant Blue G-250, 2% acetic acid and 45% methanol and then destained in a solution with 30% methanol and 10% acetic acid.

#### 2.5.2. Reverse gelatin zymography

The TIMP activity, a target-regulating MMP-2, was assayed by using a reverse gelatin zymography. Prepared culture media were electrophoresed in gel containing 0.1% gelatin and 300 ng/ml of each protein of MMP-2 and MMP-9, as described above for the gelatin zymography. The gel was incubated in a 2.5% Triton X-100 solution and was then incubated in 50 mM Tris–HCl buffer containing 200 mM NaCl, 10 mM $CaCl_2$ and 0.05% Brij-35. The gel staining and destaining followed the zymography experimental protocols as stated above. After proteolysis and staining, TIMP-2 activity was measured by densitometry of undigested bands of the appropriate molecular weights.

### 2.6. Real-time reverse transcriptase–polymerase chain reaction (RT-PCR)

The MMP-2 mRNA levels in the presence of ISL were quantitatively determined using real-time RT-PCR. Total RNA was isolated from HUVECs using a commercially available Trizol reagent kit (Gibco BRL, Gaithersburg, MD) after culture protocols according to our previous studies [14] and was reversibly transcribed using SuperScript II RT (Gibco Life Technologies, Grand Island, NY). Quantitative real-time RT-PCR technique was performed in a Rotor-Gene 3000 PCR (Corbett Life Science, Sydney, Australia) using the SYBR-green fluorescence quantification system (Qiagen, Valencia, CA) to quantify amplicons. The primer pairs (Bioneer, Korea) were as follows: MMP-2, forward: 5′-TGGCAAGTACGGCTTCTGTC-3′, reverse: 5′-TTCTTGTCGCGGTGCTAGTC-3′; glyceraldehyde-3-phosphate dehydrogenase (GAPDH), forward: 5′-GAAGGTGAAGGTCGGAGTC-3′, reverse: 5′-GAA-GATGGTGATGGGATTTC-3′. The housekeeping gene GAPDH was used for internal normalization. The standard PCR conditions were 94°C for 5 min and then 35 cycles at 94°C (20 s), 56°C (15 s) and 72°C (20 s), followed by the melting curve analysis. PCR conditions were optimized with regard to efficiency of amplification of target genes and housekeeping gene control. The absence of contaminants was confirmed by the RT-PCR assay of RNA transcript

samples without a primer addition. The progress of the PCR amplification was monitored in real time by fluorescent measurement during each amplification cycle for the expression of the target gene with normalization to the housekeeping gene. The data analysis of PCR results and calculation of the relative concentrations were performed using the Rotor-Gene software version 6.0.

### 2.7. Immunocytochemistry

After HUVECs grown on 24-well chamber slides were thoroughly washed with PBS containing 0.05% Tween 20, cells were fixed with 4% ice-cold formaldehyde for 15 min. For blocking any nonspecific binding, cells were incubated for 3 h with 1% bovine serum albumin. After washing fixed cells with PBS, polyclonal goat anti-human MT-1 MMP antibody in PBS containing 0.05% Tween 20 was incubated overnight at 4°C. Cells were incubated with cyanine-3-conjugated anti-goat IgG (Rockland, Gilbertsville, PA) as a secondary antibody. Images were obtained using an Olympus BX51 fluorescent microscope with differential interference contrast and reflected light fluorescence.

### 2.8. Cell transmigration assay

This study investigated whether ISL blocked the PMA-activated HUVEC transmigration of HUVECs cultured on the transwell chamber with a gelatin-coated filter. This transmigration assay was performed in an 8-μm-pore transwell chamber (Costar, Corning, NY). Cells were resuspended in a serum-free medium containing 50 ng/ml PMA and seeded at 60,000 cells/well on gelatin-coated filters. Cells transmigrated onto the lower surface of the filter were stained with toluidine blue, and cells migrated for 24 h were counted and photographed in the two to three microscopic fields per well using microscopy with CCD camera (Motic, Wetzlar, Germany).

### 2.9. Endothelial cell motility

An inhibitory role of ISL in the endothelial cell motility was assessed using an in vitro scratch assay. HUVECs (60,000 cells) were seeded onto a 24-well plate and incubated for 24 h in a complete medium containing 10% FBS. For the in vitro scratch assay, HUVECs were then scratched away

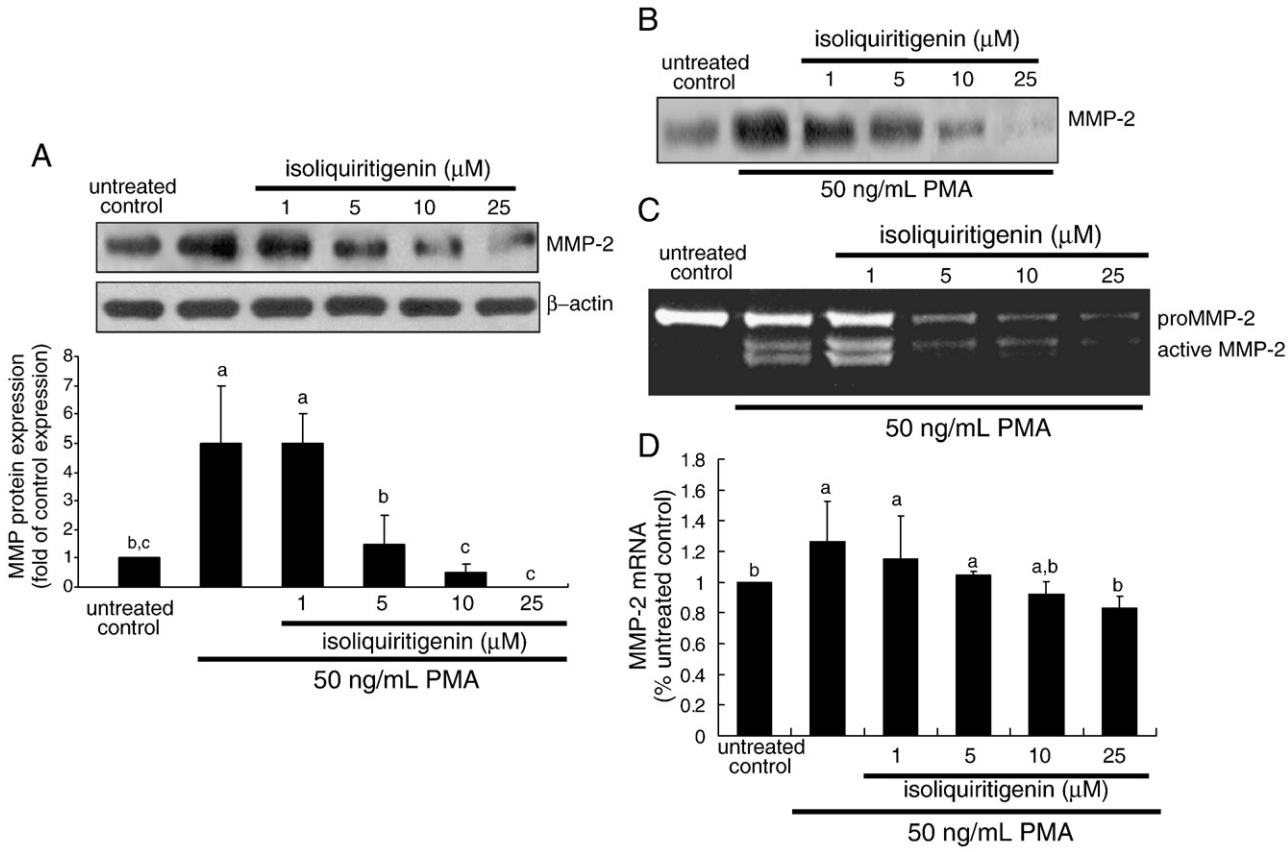


Fig. 2. Expression (A), secretion (B), gelatinolytic activity (C) and mRNA level (D) of MMP-2. After HUVEC culture protocols with 1–25 μM ISL and 50 ng/ml PMA for 24 h, equal amounts of cell lysate proteins and equal volumes of culture media were subjected to 10% SDS-PAGE and Western blot analysis (A and B) with a primary antibody against proMMP-2 (three separate experiments). β-Actin protein was used as an internal control for cellular expression of proMMP-2. The bar graphs (means±S.E.M., $n$=3) represent quantitative densitometric results of upper bands (A). Values not sharing a letter are significantly different at $P<.05$. Collected culture media were subjected to Western blot analysis (B) and gelatin zymography (C) for the enzyme activity of MMP-2. Gelatinolytic activities were detected as unstained bands against the background of Coomassie-blue-stained gelatin. MMP-2 mRNA was analyzed from cells treated with 1–25 μM ISL and 50 ng/ml PMA by semiquantitative real-time PCR (D).

horizontally on each well using a P100 pipette tip. After scratching, injured cells were incubated for another 24 h in a new medium with 50 ng/ml PMA and/or ISL. Images of the scratches were captured for five random microscopic fields of view along the scratch per treatment. A reduction in the scratched area indicates a sign of cell migration.

### 2.10. Tube formation assay

Next, we tested the role of ISL in PMA-induced HUVEC tube formation using a tubular morphogenesis assay. Matrigel Basement Membrane Matrix (BD Biosciences, Heidelberg, Germany) was used as substrate for the in vitro study of angiogenesis. The Matrigel was thawed overnight at 4°C and mixed to homogeneity in a culture medium and was allowed to solidify in a sterile environment for 24 h. HUVECs were harvested by trypsinization, and 100,000 cells per well were seeded onto 24-well plates on which 100 μl Matrigel (1:1 dilution) was distributed and incubated for 1 h at 37°C to gelatinize. The branching points were continuously monitored, and the tube formation of cells was photographed in five random fields of view per well using Motic microscopy.

### 2.11. Data analysis

Values were represented as means±S.E.M. of separate experiments. Statistical analyses were conducted using Statistical Analysis Systems statistical software package (SAS Institute, Cary, NC). Significance was determined by one-way ANOVA followed by Duncan multiple range test for multiple comparisons, and $P$ values less than .05 were considered statistically significant.

## 3. Results

### 3.1. Inhibitory effects of ISL on production of MMP-2

ISL at 1–25 μM showed no endothelial cytotoxicity in the presence of PMA, as evidenced by MTT assay (Fig. 1B). Western blot analysis was used to address the fact that 1–25 μM ISL suppressed induction of MMP-2 stimulated by PMA for 24 h in serum-free conditions (Fig. 2). As expected, PMA strikingly elevated cellular expression and secretion of MMP-2, which was reversed by ≥5 μM ISL in a dose-dependent manner (Fig. 2A and B). When cells that were exposed to PMA for 24 h were treated with ≥5 μM ISL,

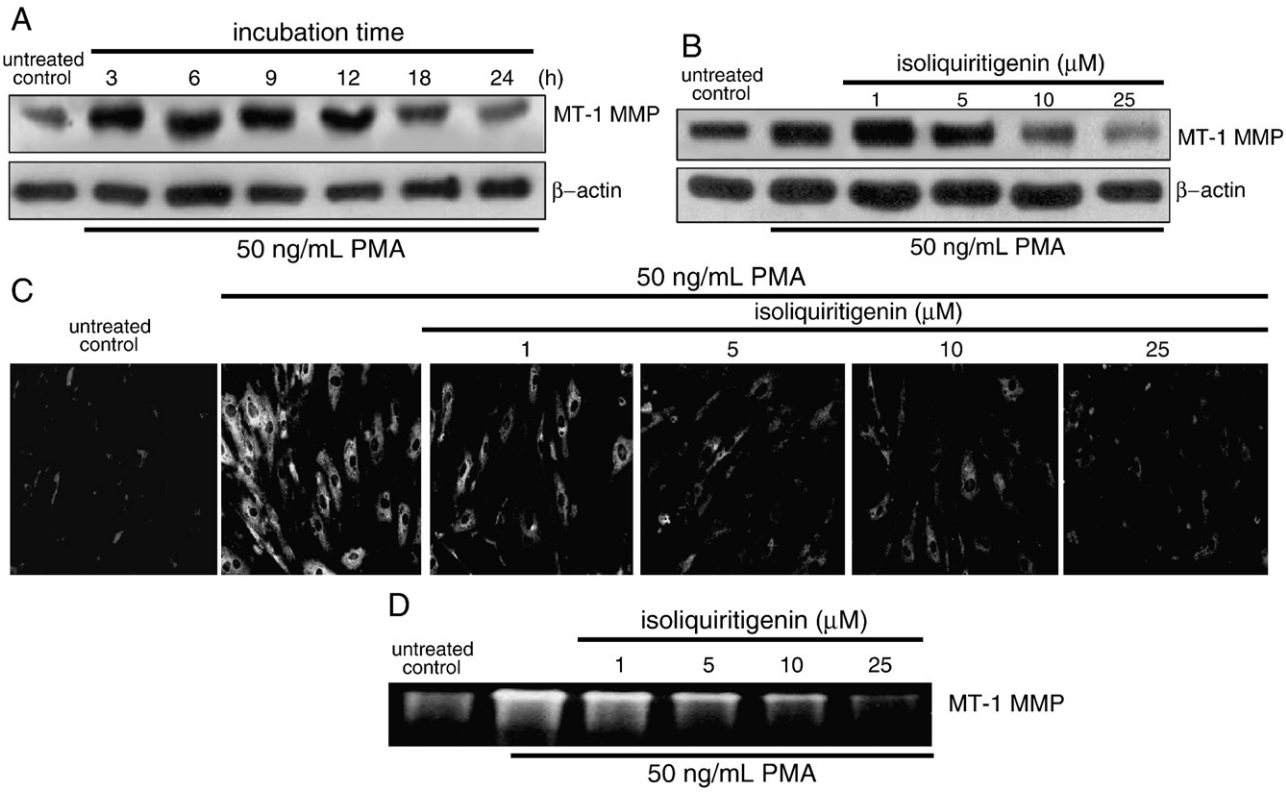


Fig. 3. Western blot data showing time-course-dependent cellular MT-1 MMP expression (A) and ISL inhibition of its expression (B) in HUVECs treated with 50 ng/ml PMA for 3–24 h. Cell lysates were subjected to electrophoresis on 10% SDS-PAGE, followed by Western blot analysis with a primary antibody against MT-1 MMP. Immunocytochemical staining (C) also detected cellular expression of MT-1 MMP in PMA-exposed human endothelial cells. Cells were fixed and then incubated with goat anti-human MT-1 MMP. Antibody localization was detected with cyanine-3-conjugated anti-goat IgG using fluorescence microscopy with rhodamine green filter. Magnification: ×400. Fibrinolytic activity of MT-1 MMP in culture media was determined by fibrin zymography (D). HUVECs were incubated with 50 ng/ml PMA for 6 h in the presence of 1–25 μM ISL. Cell lysates were subjected to fibrin zymography using 10% SDS-PAGE copolymerized with 0.1% fibrinogen and 1 U/ml thrombin. Fibrinolytic activities were detected as unstained bands against the background of Coomassie-blue-stained gelatin.

gelatin zymography revealed that the proteolytic activity of MMP-2 was nearly abolished (Fig. 2C). It was found that PMA exposure for 18 h elicited MMP-2 transcript levels substantially (Fig. 2D). ISL dampened the expression of MMP-2 mRNA in a dose–response manner, and at ≥10 μM, its expression was nearly abolished.

### 3.2. ISL inhibition of MT-1 MMP induction

Western blot analysis was used to address the fact that 1–25 μM ISL blocked the PMA-stimulated cellular expression of MT-1 MMP. Expression of this protein was elevated at 3 h after PMA activation with a >25-fold increase in stimulated cells over the untreated quiescent cells and remained high up to 12 h (Fig. 3A). ISL at ≥10 μM proved a full inhibition of MT-1 MMP induction in PMA-exposed HUVECs (Fig. 3B). In addition, immunofluorescence staining was observed in PMA-treated HUVECs, indicating augmented expression of MT-1 MMP (Fig. 3C). In contrast, ≥10 μM ISL diminished the immunofluorescence staining. To achieve the full inhibitory effect of ISL in the MT-1 MMP expression model, doses of 10–25 μM were required.

Fibrinolytic activity of MT-1 MMP was enhanced by adding PMA to HUVECs, as detected by fibrin zymography (Fig. 3D). When 1–25 μM ISL was treated with PMA-activated cells, this enzyme activity was dose-dependently attenuated with inhibitory doses being ≥5 μM. Consistently, the MMP-2 activity enhanced by PMA was markedly attenuated in PMA-exposed cells treated with ≥5 μM ISL (Fig. 2C).

### 3.3. Retardation of PMA-induced transmigration by ISL

An inhibitory role of ISL in the endothelial cell motility was assessed using a transmigration assay. This study investigated whether ISL blocked the PMA-activated

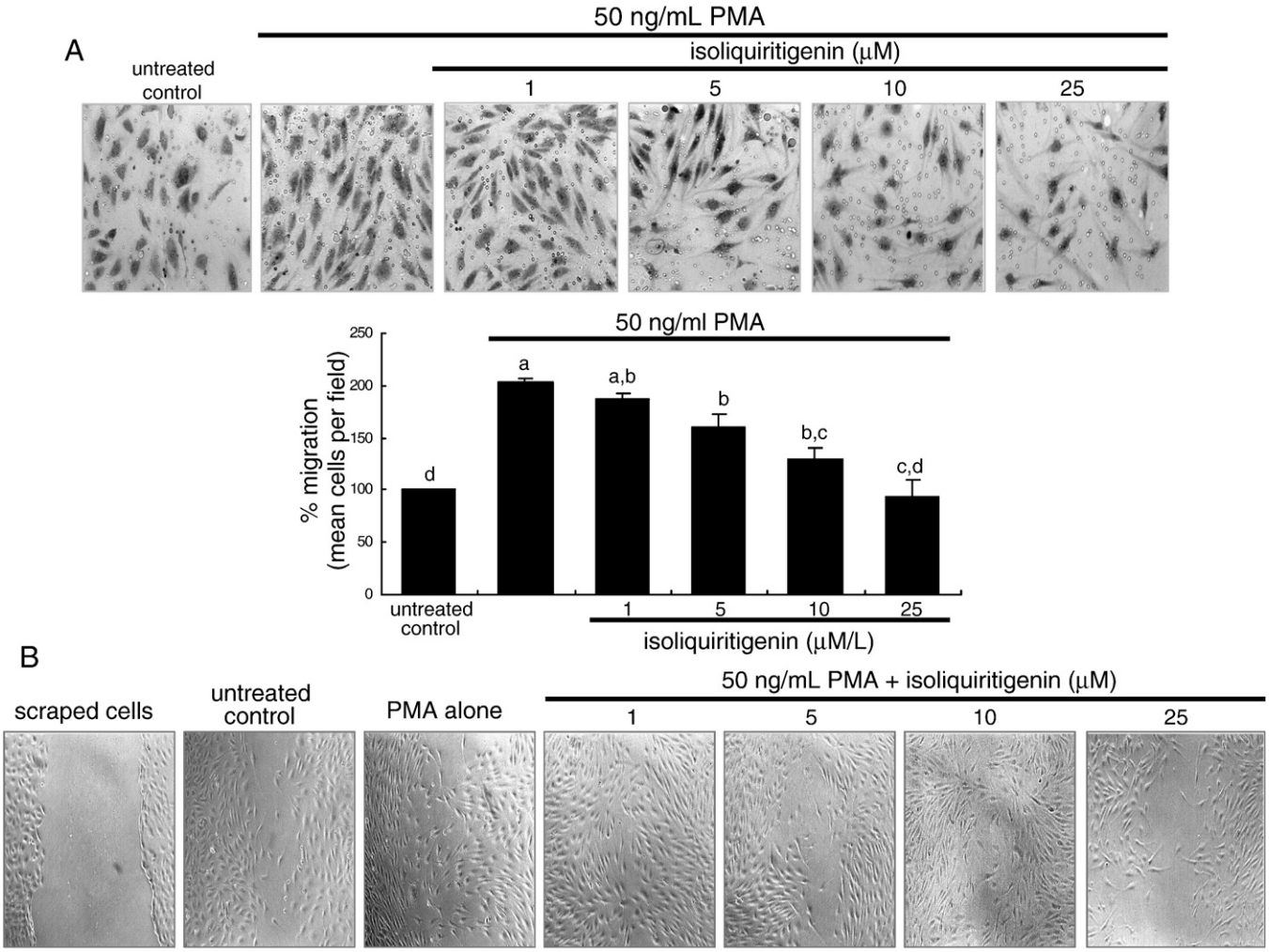


Fig. 4. ISL inhibition of cell transmigration (A) and mobility (B) in PMA-treated endothelial cells. HUVECs were cultured on gelatin-coated filters of 8-μm-pore transwells. Cells transmigrated for 24 h onto the lower surface of the filter were stained with toluidine blue and counted (A). The bar graph (means±S.E.M., $n$=4) represents the numbers of cells transmigrated. Values not sharing a letter are significantly different at $P$<.05. HUVECs were scratched away horizontally using a pipette tip. After scratching, cells were incubated for another 24 h in a new medium containing 50 ng/ml PMA and/or 1–25 μM ISL. The scratched area of each well was photographed (B).

transmigration of HUVECs cultured on the transwell chamber with a gelatin-coated filter. The addition of PMA to endothelial cells substantially promoted endothelial transmigration (Fig. 4A). In contrast, ≥5 μM ISL significantly retarded transmigration in PMA-stimulated endothelial cells. To examine inhibitory effects of ISL on endothelial cell motility, an in vitro scratch assay was performed on a confluent monolayer of HUVECs. PMA promoted the scratch recovery at 12 h postinjury, and the recovery did not occur in the presence of ≥5 μM ISL (Fig. 4B). It is deemed that MMP's degradation of ECM and basement membrane played an important role in the endothelial migration, and its activity modulated endothelial cell motility. In this study, the MMP data from Western blot and zymography (Figs. 2 and 3) supported the migration data (Fig. 4).

### 3.4. Reduction of PMA-induced tube formation by ISL

Next, we tested the role of ISL in PMA-induced HUVEC tube formation using a tubular morphogenesis assay. As expected, PMA led to the formation of tubelike structures after 12 h treatment (Fig. 5). ISL added to cells treated with PMA effectively abrogated the width and the length of endothelial tubes at doses ≥10 μM, indicating a reduction of the angiogenic activity. Accordingly, it is deemed that ISL may prevent ECM degradation and concomitantly inhibit endothelial cell organization into the vascular network through new vessel formation under tumorigenic conditions [4,5].

### 3.5. Effect of ISL on TIMP-2 level

The potential effect of ISL on TIMP-2, an alternative target encompassing the ability to regulate MMP-2 activity, was investigated by Western blot (Fig. 6A). The protein expression of TIMP-2 was elevated in endothelial cells exposed to 50 ng/ml PMA for 18 h. HUVECs treated with ISL at doses ≤10 μM showed a further increase in TIMP-2 expression, whereas 25 μM ISL dampened TIMP-2 expression induced by PMA, showing a biphasic effect on TIMP-2 expression. To determine whether ISL regulates the activity of TIMP that inhibits MMP-2, we detected TIMP-2 in media by reverse gelatin zymography (Fig. 6B). The profile of TIMP production in the presence of PMA and ISL was similar to that of cellular expression of TIMP-2. There was a higher TIMP-2 level in culture media of PMA-treated HUVECs, compared to that of untreated cells. When PMA-exposed cells were treated with ISL at nontoxic doses of 1–25 μM, the TIMP-2 production was additionally enhanced.

### 3.6. Disturbance of MAPK signaling by ISL

This study attempted to determine whether activation of JNK and p38 MAPK was involved in PMA-stimulated

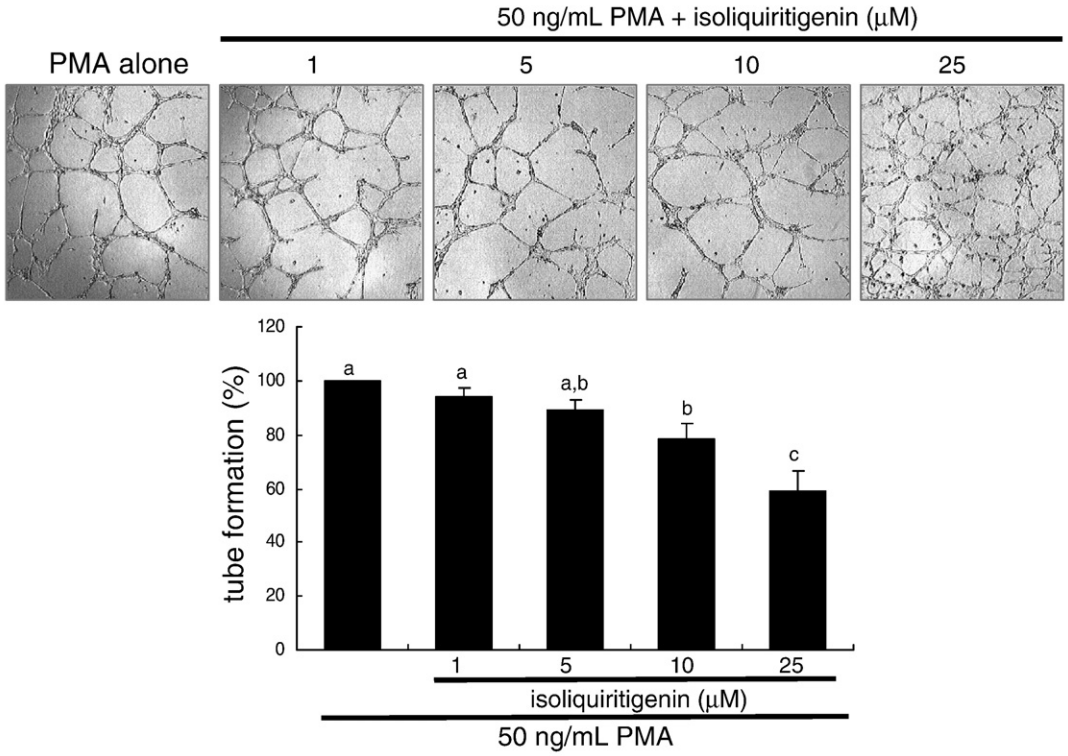


Fig. 5. Representative images showing ISL reduction of tube formation in PMA-treated endothelial cells plated onto Matrigel. After 12 h of incubation with 1–25 μM ISL, cells were fixed and images at ×100 magnification were captured. From the image, the number of tubes was determined. Multiple five random fields of view were analyzed for the quantitative results. Tube formation results are plotted as means±S.E.M. ($n$=4) for each group. Values not sharing a letter are significantly different at $P$<.05.

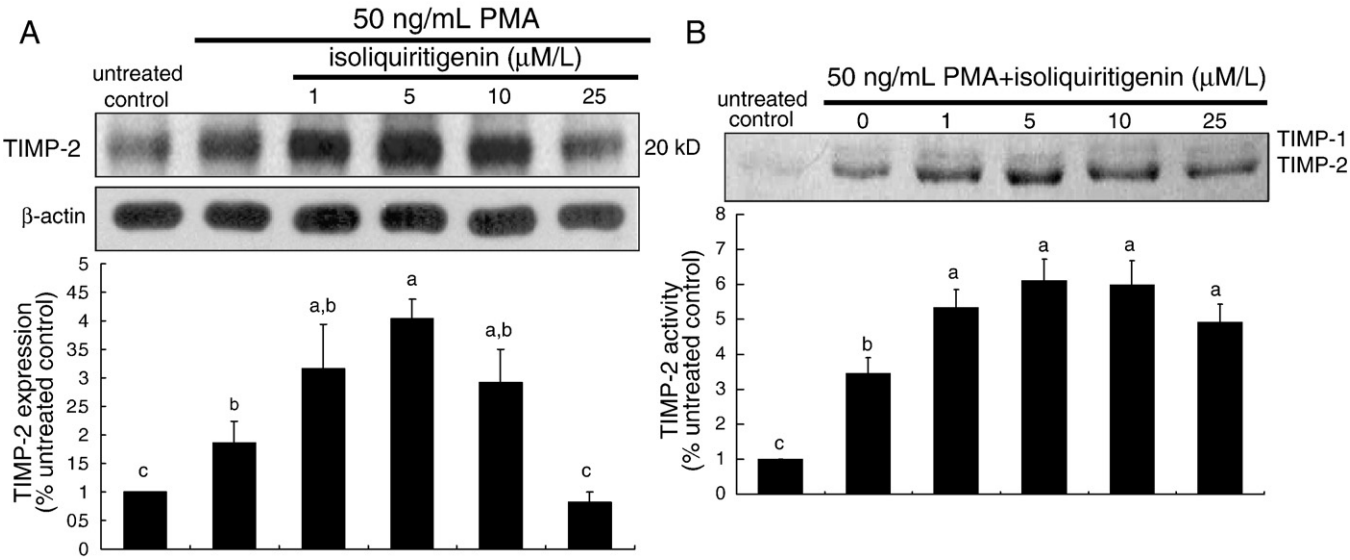


Fig. 6. Effects of ISL on cellular protein expression (A) and production of TIMP-2 (B) from HUVECs exposed to PMA and ISL for 18–24 h. After HUVEC culture protocols, cell lysates were subjected to 8% SDS-PAGE and Western blot analysis with a primary antibody against TIMP-2 (A). β-Actin protein was used as an internal control for cellular expression of TIMP-2. The bar graphs (means±S.E.M., $n$=3) represent quantitative densitometric results of upper bands (A). HUVEC-conditioned medium in the presence of 50 ng/ml PMA and/or ISL was subjected to reverse gelatin zymography (B). TIMP activity was detected as Coomassie-blue-stained bands against the background of unstained gel. Representative reverse zymograms were plotted as means±S.E.M. ($n$=3). Values not sharing a letter are significantly different at $P$<.05.

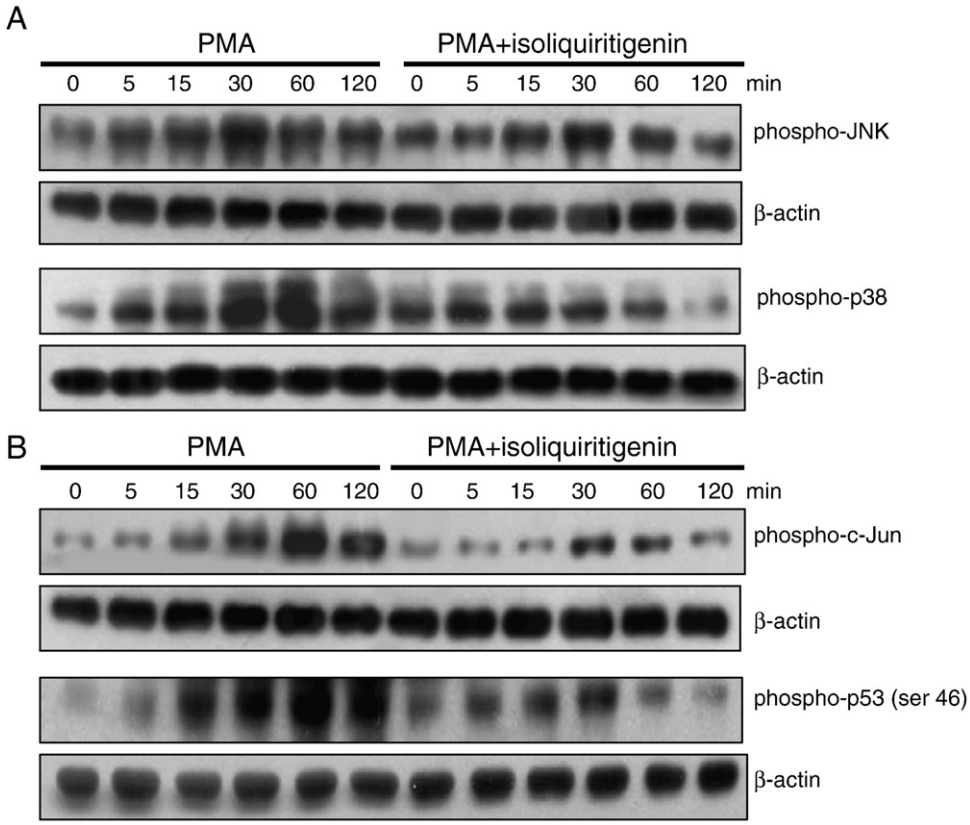


Fig. 7. Time-course inhibition by ISL of phosphorylation of JNK and p38 MAPK (A) and of activation of c-Jun and p53 (B) in PMA-exposed HUVECs. Confluent cells were exposed to 50 ng/ml PMA in the presence of 25 μM ISL. Total cell protein extracts were electrophoresed, followed by Western blot analysis with a primary antibody against each protein (three independent experiments). β-Actin protein was used as an internal control.

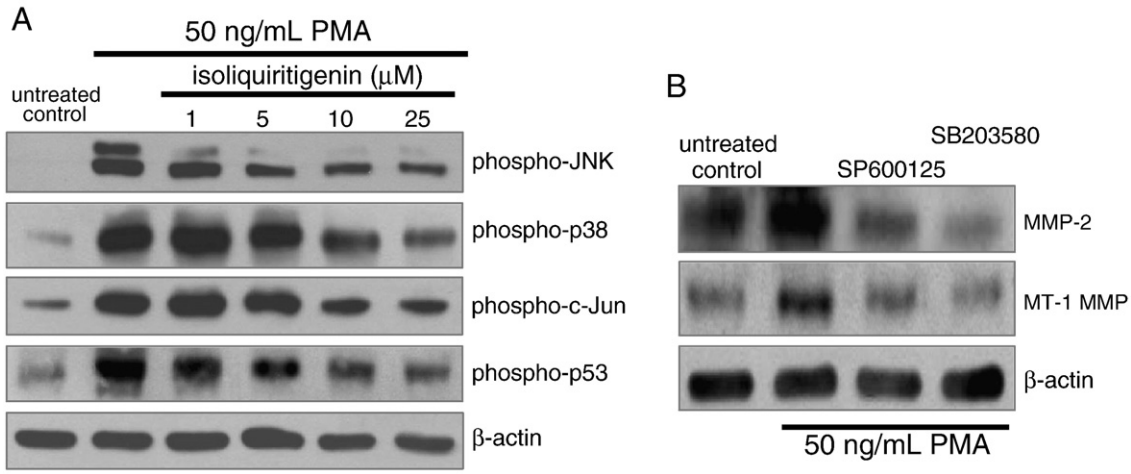


Fig. 8. Dose-responsive inhibition by ISL of phosphorylation of JNK, c-Jun, p38 MAPK and p53 in PMA-exposed HUVECs (A), and cellular expression of MMP-2 and MT-1 MMP in the presence of a JNK inhibitor and a p38 MAPK inhibitor (B). Confluent cells were exposed to 50 ng/ml PMA in the presence of 1–25 μM ISL (A). Total cell lysates were electrophoresed, followed by Western blot analysis with a primary antibody against each protein (three independent experiments). β-Actin protein was used as an internal control. Cells were treated with 10 μM JNK inhibitor or p38 MAPK inhibitor and then exposed to 50 ng/ml PMA (B). Electrophoresis and Western blot analysis were run for expression of MMP-2 and MT-1 MMP.

angiogenic activity via MMP activation and whether ISL was able to block these MAPK-responsive signaling pathways (Figs. 7 and 8). PMA rapidly induced phosphorylation of JNK and p38 MAPK within 30 min incubation, while 25 μM ISL nearly completely blocked the activation of JNK and p38 MAPK (Fig. 7A). The involvement of the kinase cascades was next elucidated in the angiogenesis process. Western blot analysis revealed a marked increase in the active phosphorylated forms of c-Jun and p53, respective downstream effectors of JNK and p38 MAPK, in PMA-treated endothelial cells (Fig. 7B). As expected, ISL elicited a marked reduction of PMA-induced activation of both c-Jun and p53 within 15–30 min.

Whether ISL abrogated activation of p38 and JNK MAPK pathways involved in the angiogenesis process was further investigated (Fig. 8A). PMA-triggered activation of JNK and p38 MAPK subsided in endothelial cells treated with ≥10 μM ISL. In addition, ISL at doses ≥10 μM hampered signaling pathways of JNK and p38 MAPK. When the JNK inhibitor SP600125 was added, the expression of MMP-2 and MT-1 MMP was attenuated (Fig. 8B). Additionally, SB203580, a specific inhibitor of p38 MAPK, reduced both MMP-2 and MT-1 MMP protein levels in endothelial cells, targeting both JNK and p38 MAPK as activators of proteolysis.

## 4. Discussion

Five major findings were observed in this study.

1. When ISL at the nontoxic doses of 1–25 μM was added to cells, endothelial production and gelatinolytic activity of MMP-2 elevated by PMA were substantially mitigated in a dose-dependent manner at transcriptional levels.
2. PMA enhanced expression and fibrinolytic activity of MT-1 MMP, whereas ISL attenuated its activation, most likely responsible for MMP-2 activity.
3. ISL at ≥5 μM dampened PMA-stimulated migration and tube formation of endothelial cells. It is deemed that MMP's degradation of ECM and basement membrane plays an important role in the endothelial migration, and its activity modulated endothelial cell motility.
4. PMA-exposed and ISL-treated cells showed higher levels of TIMP compared to PMA-alone cells.
5. ISL disturbed PMA-triggered switch-on of MAPK signaling pathways leading to MMP production. These overall observations demonstrate that ISL, a licorice component, has the potential to prevent angiogenesis, inflammation and atherosclerosis involving ECM degradation. The ability to block endothelial MMP secretion argues for a therapeutic target of actions of ISL under various pathological conditions.

Previous studies have shown that polyphenolic compounds rich in fruits and vegetables have substantial antioxidant abilities under various oxidative circumstances [21]. Recent studies have focused on mechanisms by which polyphenols may confer cardiovascular protection, inhibition of angiogenesis and cell migration in blood vessels [22,23]. The mechanisms triggered by polyphenols with specific structures contribute to a variety of vascular functions such as antiangiogenic, antiatherogenic, vasorelaxant and antihypertensive effects observed in experimental animals and in clinical patients [22]. In addition, there are multiple targets for the cancer chemoprevention by green tea and its polyphenolic constituents by modulating novel pathways involved in angiogenesis and metastasis [23,24]. There has been much intensive interest in the beneficial

health actions of bioactive compounds present in licorice plant [13,25]. In vitro studies have shown that ISL induces apoptosis in various cancer cells as a promising potential chemopreventive agent [15,17]. Licorice-derived flavonoids including ISL, isoliquiritin and liquiritigenin inhibited tube formation from vascular endothelial cells and granuloma angiogenesis [18]. Consistently, this study showed that submicromolar ISL abrogated PMA-triggered endothelial migration and tube formation. However, the antitumor mechanisms of ISL have not been well defined.

There is little literature regarding MMP's involvement in matrix modification of ISL as a chemopreventive mechanism. It was assumed in this study that the ISL blockade of the MMP production and activation hampered endothelial cell motility. MMP was involved in the angiogenic and metastatic cascades of knockout or transgenic animals and tumor cell lines overexpressing or down-regulating a specific MMP [26–28]. One of the earliest events in cancer metastasis and angiogenesis is a proteolytic degradation of the ECM proteins including the basement membrane [26]. Accordingly, MMP has been clearly implicated for important targets of cancer therapy. Indeed, dietary botanicals such as green tea catechins and grape seed proanthocyanidins have been shown as MMP inhibitors and as chemotherapeutic agents [23,24,29]. Silibinin, a flavonoid antioxidant from milk thistle, inhibited colorectal cancer growth by inhibiting tumor cell proliferation and angiogenesis in nude mice implanted with HT29 cells [30]. The antiangiogenic effect of silibinin against colorectal carcinoma was coupled with a strong decrease in inducible nitric oxide synthase, cyclooxygenase and vascular endothelial growth factor. There is little literature regarding MMP's involvement in matrix modification of ISL as a chemopreventive or antiatherogenic mechanism. However, another licorice component, glycyrrhizin, prevented acute liver injury through down-regulation of MMP-9 in mice [31].

Several in vitro and in vivo studies have suggested the antitumor efficacy of ISL, which involves its antiproliferative, proapoptotic and antiangiogenic activities [15–18]. It was shown that the inhibition of phosphatidylinositol 3-kinase (PI3K)/Akt signaling pathway may account for the antiproliferative and proapoptotic effects of ISL [32]. However, molecular biomarkers and mechanisms for the antiangiogenic effect of ISL against tumor growth have been barely identified. This study revealed that the rapid phosphorylation of JNK and p38 MAPK in PMA-exposed HUVECs was substantially down-regulated by ISL dampening MMP activation. In addition, ISL appeared to block endothelial motility and tube formation possibly via selectively acting on JNK and p38 MAPK, which converge at the level of transcription regulation of c-Jun and p53. Accordingly, these MAPKs were believed to be components of angiogenic and tumorigenic pathways triggered by phorbol ester, and the ISL inhibition of these MAPK pathways exhibited antiangiogenic efficacy. Silibinin has been found to inhibit PMA-induced MMP-9 transcription activity and cancer cell invasion by blocking the activation of AP-1 via MAPK signaling pathways [33]. Flavanone rich in citrus may perturb the invasion and metastasis of lung cancer cells with reduced expressions of MMP-2 and uPA through inactivation of extracellular signal-regulated kinase 1/2 and p38 MAPK signaling pathways [34]. Additionally, treatment with grape seed proanthocyanidins inhibited MMP-9 expression in human epidermoid carcinoma A431 cells via mitigating PI3K levels and Akt phosphorylation, suggesting that this compound might be effective in the treatment of skin cancers [35].

In summary, the present study has shown that the licorice component ISL suppresses expression and activity of MMP-2 and MT-1 MMP at nontoxic doses. It is deemed that the ISL inhibition of the gelatinolytic activity of MMP-2 was mediated via dampening activation of MT-1 MMP. This was responsible for blocking endothelial migration tube formation, most likely through degrading the basement membrane. The MMP production and activation may entail activation of the MAPK signaling pathways of JNK and p38, which was hampered by adding ISL. Compelling evidence that ISL has the potential to prevent angiogenesis, inflammation and atherosclerosis involving ECM degradation is drawn from this study.

## Acknowledgments

This study was supported by Grant R01-2006-000-10896-0 from Korea Science and Engineering Foundation, Grant R12-2001-047-02004-0 from Korea Science and Engineering through the Silver Biotechnology Research Center at Hallym University, Grant 10027174-2007-02 from the Ministry of Commerce, Industry and Energy and Brain Korea 21 from Korea Research Foundation.

## References

[1] Nagase H, Visse R, Murphy G. Structure and function of matrix metalloproteinases and TIMPs. Cardiovasc Res 2006;69:562–73.
[2] Dollery CM, Libby P. Atherosclerosis and proteinase activation. Cardiovasc Res 2006;69:625–35.
[3] Rodriguez-Pla A, Bosch-Gil JA, Rossello-Urgell J, Huguet-Redecilla P, Stone JH, Vilardell-Tarres M. Metalloproteinase-2 and -9 in giant cell arteritis: involvement in vascular remodeling. Circulation 2005;112:264–9.
[4] Tosetti F, Ferrari N, De Flora S, Albini A. Angioprevention: angiogenesis is a common and key target for cancer chemopreventive agents. FASEB J 2002;16:2–14.
[5] John A, Tuszynski G. The role of matrix metalloproteinases in tumor angiogenesis and tumor metastasis. Pathol Oncol Res 2001;7:14–23.
[6] Kargozaran H, Yuan SY, Breslin JW, Watson KD, Gaudreault N, Breen A, et al. A role for endothelial-derived matrix metalloproteinase-2 in breast cancer cell transmigration across the endothelial-basement membrane barrier. Clin Exp Metastasis 2007;24:495–502.
[7] Kugler A. Matrix metalloproteinases and their inhibitors. Anticancer Res 1999;19:1589–92.
[8] Das A, McGuire P. Role of urokinase inhibitors in choroidal neovascularization. Semin Ophthalmol 2006;21:23–7.

[9] Baltina LA. Chemical modification of glycyrrhizic acid as a route to new bioactive components for medicine. Curr Med Chem 2003;10: 155–71.
[10] Asano T, Ishihara K, Morota T, Takeda S, Aburada M. Permeability of the flavonoids liquiritigenin and its glycosides in licorice roots and davidigenin, a hydrogenated metabolite of liquiritigenin, using human intestinal cell line Caco-2. J Ethnopharmacol 2003;89:285–9.
[11] Fu Y, Hsieh TC, Guo J, Kunicki J, Lee MY, Darzynkiewicz Z, et al. Licochalcone-A, a novel flavonoid isolated from licorice root (*Glycyrrhiza glabra*), causes G2 and late-G1 arrests in androgen-independent PC-3 prostate cancer cells. Biochem Biophys Res Commun 2004;322:263–70.
[12] Kang JS, Yoon YD, Cho IJ, Han MH, Lee CW, Park SK, et al. Glabridin, an isoflavan from licorice root, inhibits inducible nitric-oxide synthase expression and improves survival of mice in experimental model of septic shock. J Pharmacol Exp Ther 2005; 312:1187–94.
[13] Chin YW, Jung HA, Liu Y, Su BN, Castoro JA, Keller WJ, et al. Anti-oxidant constituents of the roots and stolons of licorice (*Glycyrrhiza glabra*). J Agric Food Chem 2007;55:4691–7.
[14] Kwon HM, Choi YJ, Choi JS, Kang SW, Bae JY, Kang IJ, et al. Blockade of cytokine-induced endothelial cell adhesion molecule expression by licorice isoliquiritigenin through NF-κB signal disruption. Exp Biol Med (Maywood) 2007;232:235–45.
[15] Lee CK, Son SH, Park KK, Park JH, Lim SS, Chung WY. Isoliquiritigenin inhibits tumor growth and protects the kidney and liver against chemotherapy-induced toxicity in a mouse xenograft model of colon carcinoma. J Pharmacol Sci 2008;106:444–51.
[16] Ma J, Fu NY, Pang DB, Wu WY, Xu AL. Apoptosis induced by isoliquiritigenin in human gastric cancer MGC-803 cells. Planta Med 2001;67:754–7.
[17] Jung JI, Lim SS, Choi HJ, Cho HJ, Shin HK, Kim EJ, et al. Isoliquiritigenin induces apoptosis by depolarizing mitochondrial membranes in prostate cancer cells. J Nutr Biochem 2006;17: 689–96.
[18] Kobayashi S, Miyamoto T, Kimura I, Kimura M. Inhibitory effect of isoliquiritin, a compound in licorice root, on angiogenesis in vivo and tube formation in vitro. Biol Pharm Bull 1995;18:1382–6.
[19] Sheela ML, Ramakrishna MK, Salimath BP. Angiogenic and proliferative effects of the cytokine VEGF in Ehrlich ascites tumor cells is inhibited by *Glycyrrhiza glabra*. Int Immunopharmacol 2006; 6:494–8.
[20] Choi YJ, Jeong YJ, Lee YJ, Kwon HM, Kang YH. (−)Epigallocatechin gallate and quercetin enhance survival signaling in response to oxidant-induced human endothelial apoptosis. J Nutr 2005;135:707–13.
[21] Nijveldt RJ, van Nood E, van Hoorn DE, Boelens PG, van Norren K, van Leeuwen PA. Flavonoids: a review of probable mechanisms of action and potential applications. Am J Clin Nutr 2001;74:418–25.
[22] Stoclet JC, Chataigneau T, Ndiaye M, Oak MH, El Bedoui J, Chataigneau M, et al. Vascular protection by dietary polyphenols. Eur J Pharmacol 2004;500:299–313.
[23] Siddiqui IA, Malik A, Adhami VM, Asim M, Hafeez BB, Sarfaraz S, et al. Green tea polyphenol EGCG sensitizes human prostate carcinoma LNCaP cells to TRAIL-mediated apoptosis and synergistically inhibits biomarkers associated with angiogenesis and metastasis. Oncogene 2008;27:2055–63.
[24] Tang FY, Chiang EP, Shih CJ. Green tea catechin inhibits ephrin-A1-mediated cell migration and angiogenesis of human umbilical vein endothelial cells. J Nutr Biochem 2007;18:391–9.
[25] Visavadiya NP, Narasimhacharya AV. Hypocholesterolaemic and antioxidant effects of *Glycyrrhiza glabra* (Linn) in rats. Mol Nutr Food Res 2006;50:1080–6.
[26] Chesler L, Goldenberg DD, Seales IT, Satchi-Fainaro R, Grimmer M, Collins R, et al. Malignant progression and blockade of angiogenesis in a murine transgenic model of neuroblastoma. Cancer Res 2007;67:9435–42.
[27] Blázquez C, Salazar M, Carracedo A, Lorente M, Egia A, González-Feria L, et al. Cannabinoids inhibit glioma cell invasion by down-regulating matrix metalloproteinase-2 expression. Cancer Res 2008; 68:1945–52.
[28] Pulukuri SM, Rao JS. Matrix metalloproteinase-1 promotes prostate tumor growth and metastasis. Int J Oncol 2008;32:757–65.
[29] Katiyar SK. Matrix metalloproteinases in cancer metastasis: molecular targets for prostate cancer prevention by green tea polyphenols and grape seed proanthocyanidins. Endocr Metab Immune Disord Drug Targets 2006;6:17–24.
[30] Singh RP, Gu M, Agarwa R. Silibinin inhibits colorectal cancer growth by inhibiting tumor cell proliferation and angiogenesis. Cancer Res 2008;68:2043–50.
[31] Abe K, Ikeda T, Wake K, Sato T, Sato T, Inoue H. Glycyrrhizin prevents of lipopolysaccharide/D-galactosamine-induced liver injury through down-regulation of matrix metalloproteinase-9 in mice. J Pharm Pharmacol 2008;60:91–7.
[32] Jung JI, Chung E, Seon MR, Shin HK, Kim EJ, Lim SS, et al. Isoliquiritigenin (ISL) inhibits ErbB3 signaling in prostate cancer cells. Biofactors 2006;28:159–68.
[33] Lee SO, Jeong YJ, Im HG, Kim CH, Chang YC, Lee IS. Silibinin suppresses PMA-induced MMP-9 expression by blocking the AP-1 activation via MAPK signaling pathways in MCF-7 human breast carcinoma cells. Biochem Biophys Res Commun 2007;354:165–71.
[34] Hsiao YC, Kuo WH, Chen PN, Chang HR, Lin TH, Yang WE, et al. Flavanone and 2′-OH flavanone inhibit metastasis of lung cancer cells via down-regulation of proteinases activities and MAPK pathway. Chem Biol Interact 2007;167:193–206.
[35] Meeran SM, Katiyar SK. Proanthocyanidins inhibit mitogenic and survival-signaling in vitro and tumor growth in vivo. Front Biosci 2008;13:887–97.